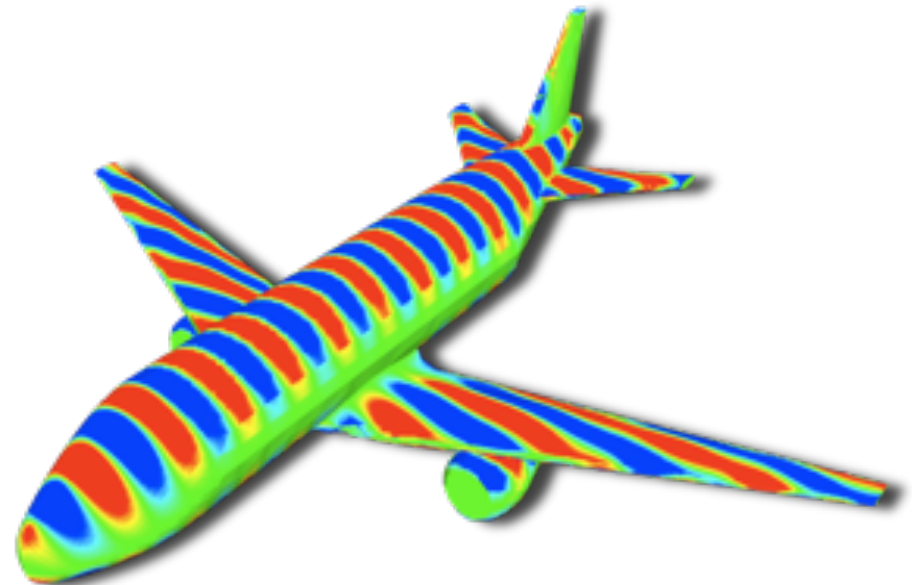
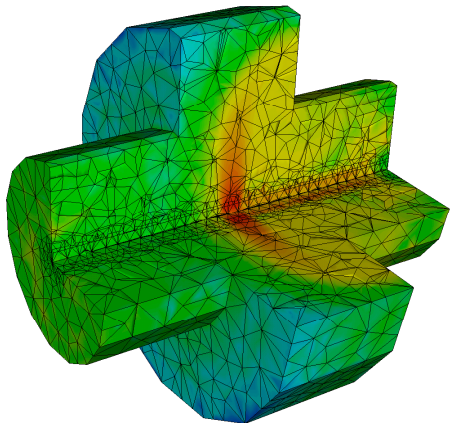

DG-FEM for PDE's

Lecture 3

Jan S Hesthaven
Brown University
Jan.Hesthaven@Brown.edu



A brief overview of what's to come

- Lecture 1: Introduction and DG-FEM in 1D
- Lecture 2: Implementation and numerical aspects
- **Lecture 3: Insight through theory**
- Lecture 4: Nonlinear problems
- Lecture 5: Extension to two spatial dimensions
- Lecture 6: Introduction to mesh generation
- Lecture 7: Higher order/Global problems
- Lecture 8: 3D and advanced topics

Lecture 3

- ✓ Let's briefly recall what we know
- ✓ Why high order methods ?
- ✓ Part I:
 - ✓ Constructing fluxes for linear systems
 - ✓ Approximation theory on the interval
- ✓ Part II:
 - ✓ Convergence and error estimates
 - ✓ Dispersive properties
 - ✓ Discrete stability and how to overcome

Let us recall

We already know a lot about the basic DG-FEM

- **Stability** is provided by carefully choosing the numerical flux.
- **Accuracy** appear to be given by the local solution representation.
- We can utilize major advances on **monotone schemes** to design fluxes.
- The scheme generalizes with very few changes to very general problems -- **multidimensional systems of conservation laws**.

Let us recall

We already know a lot about the basic DG-FEM

- **Stability** is provided by carefully choosing the numerical flux.
- **Accuracy** appear to be given by the local solution representation.
- We can utilize major advances on **monotone schemes** to design fluxes.
- The scheme generalizes with very few changes to very general problems -- **multidimensional systems of conservation laws**.

At least in principle -- but what can we actually prove ?

Why high-order accuracy ?

Let us just make sure we understand why high-order accuracy/methods is a good idea

General concerns/criticism:

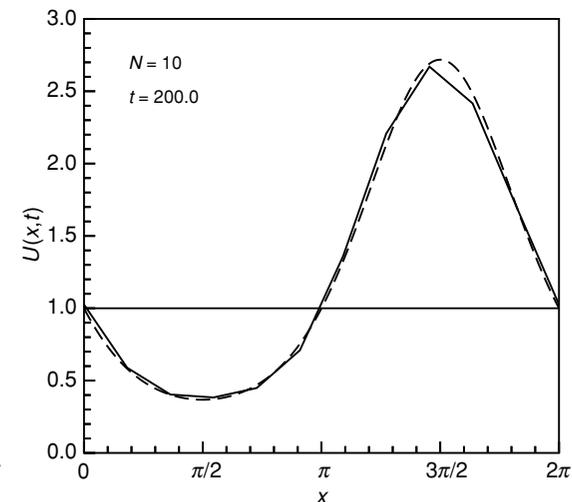
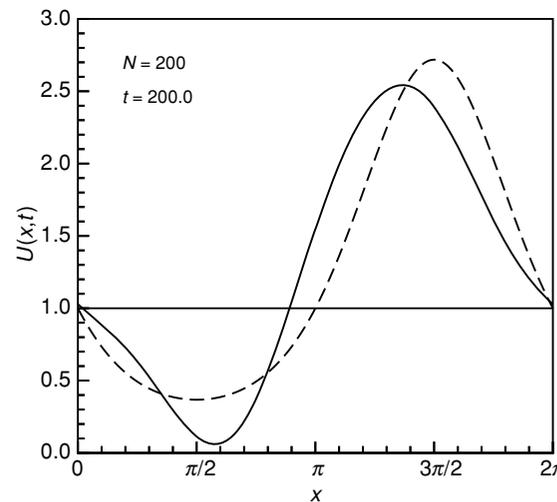
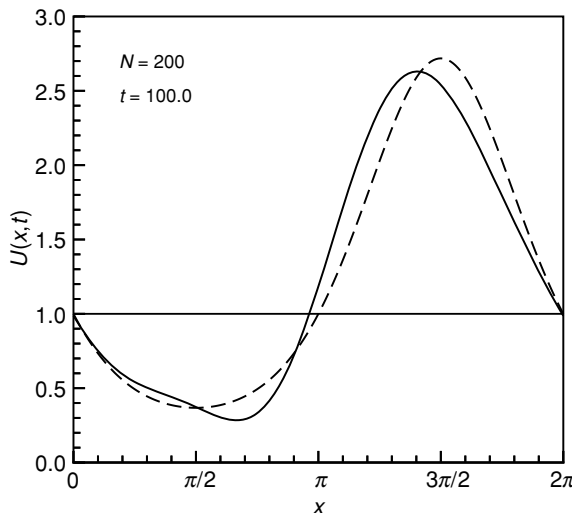
- ▶ High-order accuracy is not needed for real appl.
- ▶ The methods are not robust/flexible
- ▶ They only work for smooth problems
- ▶ They are hard to do in complex geometries
- ▶ They are too expensive

*After having worked on these methods
for 15 years, I have heard them all*

Why high-order accuracy ?

How do I solve a wave-problem to a given accuracy, , for a specific period of time, , most efficiently ?

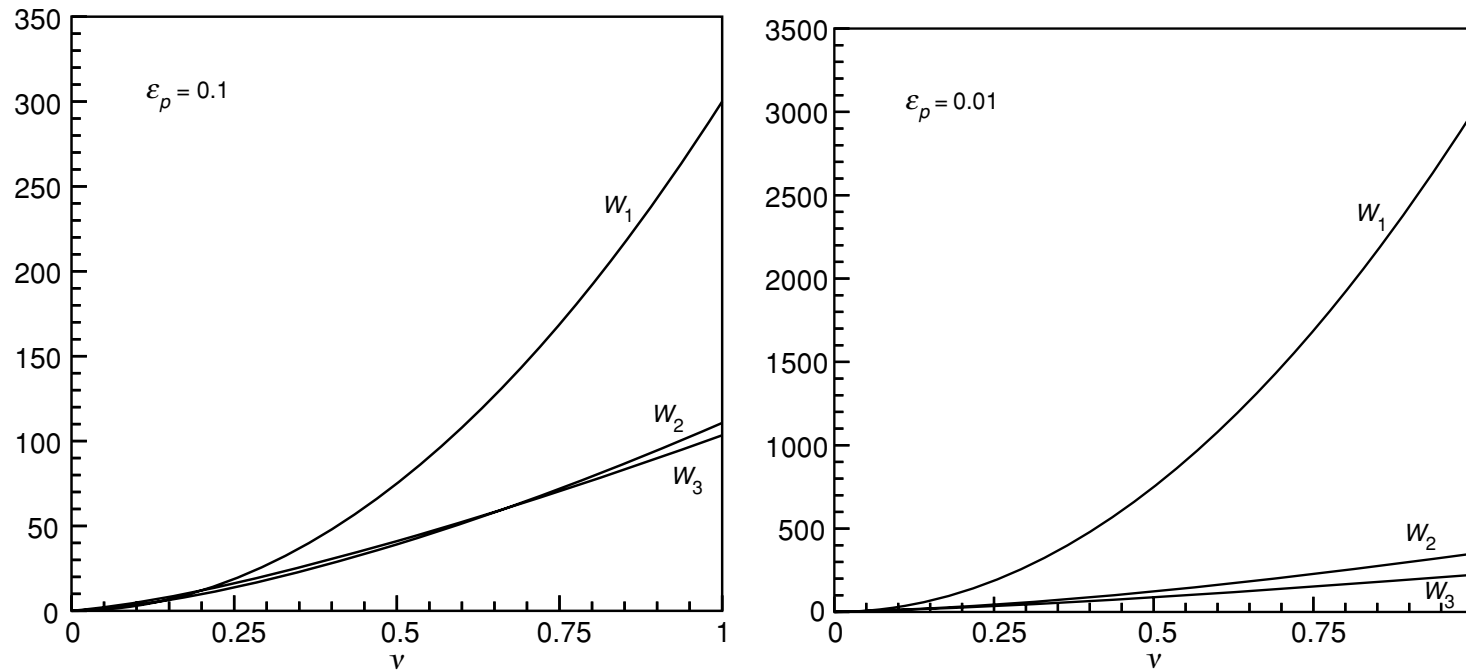
$$\text{Memory} \propto \left(\frac{\nu}{\varepsilon_p} \right)^{\frac{d}{2m}}, \quad \text{Work} \propto (2m)^d \nu \left(\frac{\nu}{\varepsilon_p} \right)^{\frac{d+1}{2m}}$$



2nd order FD

Infinite order FD

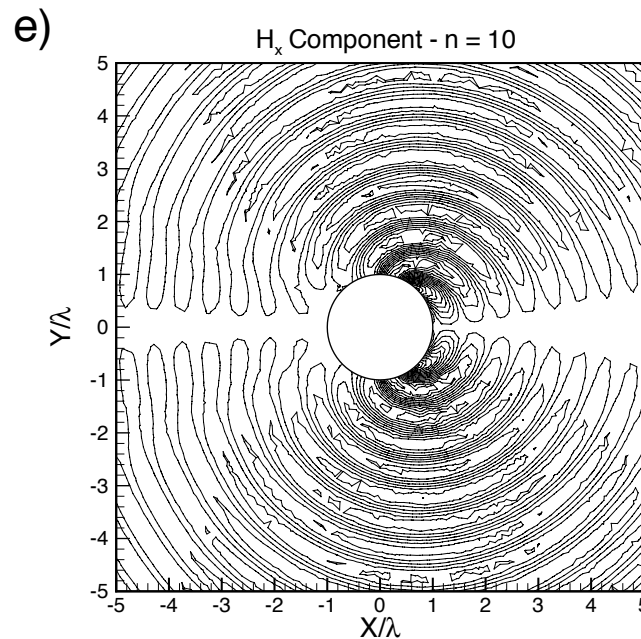
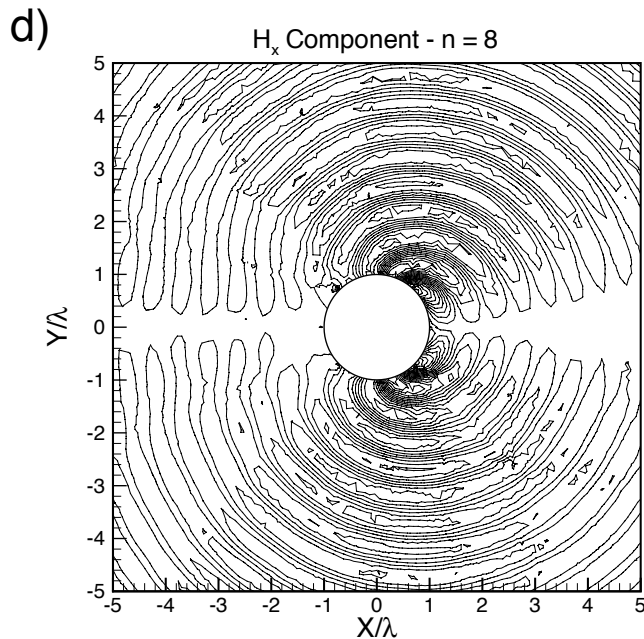
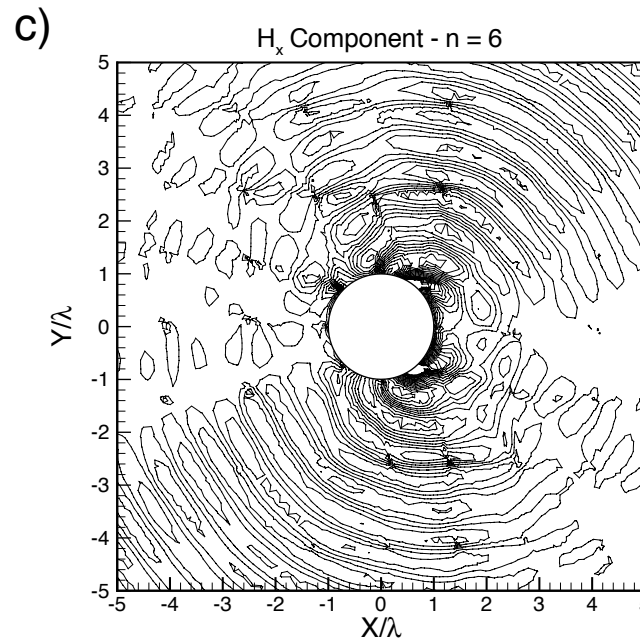
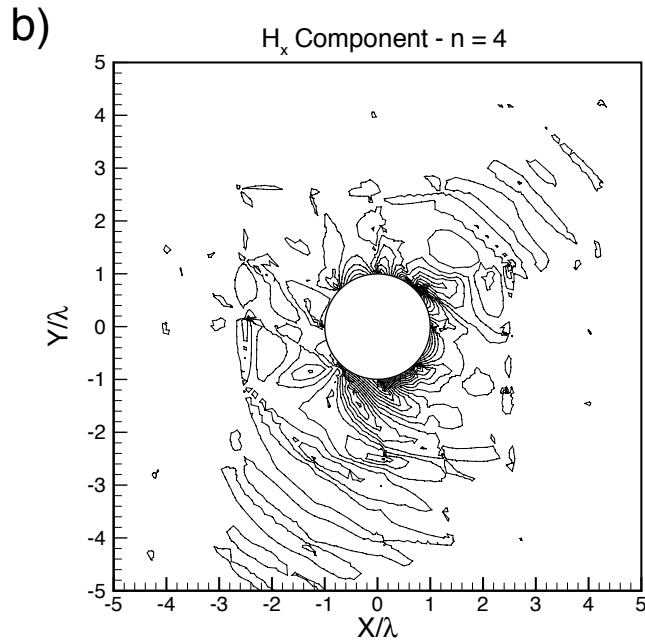
Why high-order accuracy ?



High-order is important if

- ▶ High accuracy is required - and it increasingly is !
- ▶ Long time integration is needed
- ▶ High-dimensional problems (3D) are considered
- ▶ Memory restrictions become a bottleneck

Added benefit of high-order support



High-order
takes 'some' of
the pain out of
grid generation

But first a bit more on fluxes

Let us briefly look a little more carefully at linear systems

$$Q(\mathbf{x}) \frac{\partial u}{\partial t} + \nabla \cdot \mathcal{F} = Q(\mathbf{x}) \frac{\partial u}{\partial t} + \frac{\partial F_1}{\partial x} + \frac{\partial F_2}{\partial y} = 0,$$

$$\mathcal{F} = [F_1, F_2] = [A_1(\mathbf{x})u, A_2(\mathbf{x})u].$$

Prominent examples are

- Acoustics
- Electromagnetics
- Elasticity

In such cases we can derive *exact upwind* fluxes

Linear systems and fluxes

Assume first that all coefficients vary smoothly

$$Q(\mathbf{x}) \frac{\partial \mathbf{u}}{\partial t} + \mathcal{A}_1(\mathbf{x}) \frac{\partial \mathbf{u}}{\partial x} + \mathcal{A}_2(\mathbf{x}) \frac{\partial \mathbf{u}}{\partial y} + \mathcal{B}(\mathbf{x}) \mathbf{u} = 0,$$

The flux along a normal $\hat{\mathbf{n}}$ is then

$$\Pi = (\hat{n}_x \mathcal{A}_1(\mathbf{x}) + \hat{n}_y \mathcal{A}_2(\mathbf{x})). \quad \hat{\mathbf{n}} \cdot \mathcal{F} = \Pi \mathbf{u}.$$

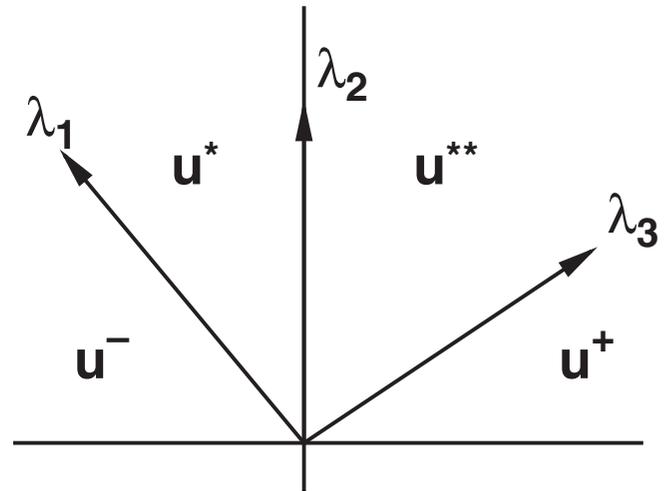
Now diagonalize this as

$$Q^{-1} \Pi = \mathcal{S} \Lambda \mathcal{S}^{-1},$$

$$\Lambda = \Lambda^+ + \Lambda^-,$$

and we obtain

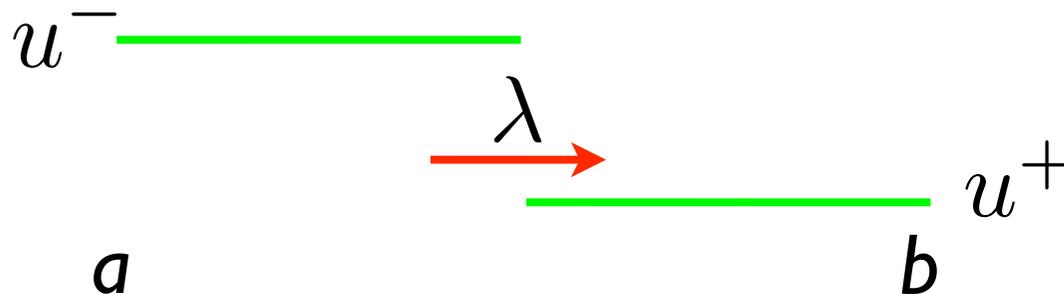
$$(\hat{\mathbf{n}} \cdot \mathcal{F})^* = Q \mathcal{S} (\Lambda^+ \mathcal{S}^{-1} \mathbf{u}^- + \Lambda^- \mathcal{S}^{-1} \mathbf{u}^+),$$



Linear systems and fluxes

For non-smooth coefficients, it is a little more complex

Consider the problem $\frac{\partial u}{\partial t} + \lambda \frac{\partial u}{\partial x} = 0, \quad x \in [a, b].$



Then we clearly have

$$\frac{d}{dt} \int_a^b u \, dx = -\lambda (u(b, t) - u(a, t)) = f(a, t) - f(b, t),$$

$$\frac{d}{dt} \int_a^b u \, dx = \frac{d}{dt} ((\lambda t - a)u^- + (b - \lambda t)u^+) = \lambda(u^- - u^+).$$

Linear systems and fluxes

Hence, by simple mass conservation, we achieve

$$-\lambda(u^- - u^+) + (f^- - f^+) = 0.$$

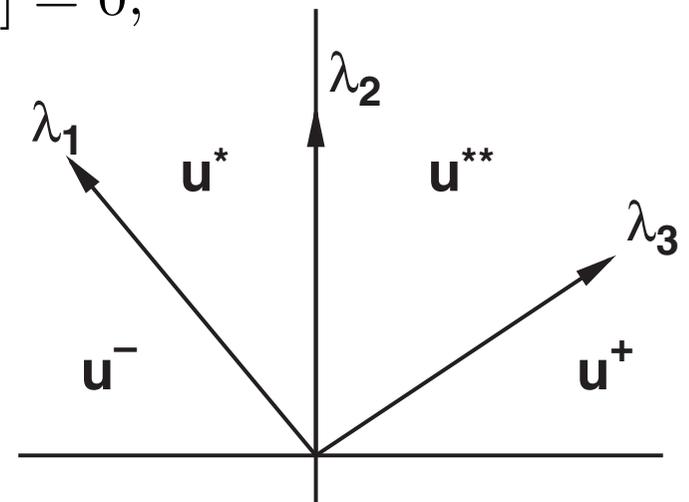
for $a \rightarrow x^-, b \rightarrow x^+$

These are the **Rankine-Hugoniot conditions**

For the general system, these are

$$\forall i : -\lambda_i Q[u^- - u^+] + [(Hu)^- - (Hu)^+] = 0,$$

They must hold across each wave and can be used to connect across the interface



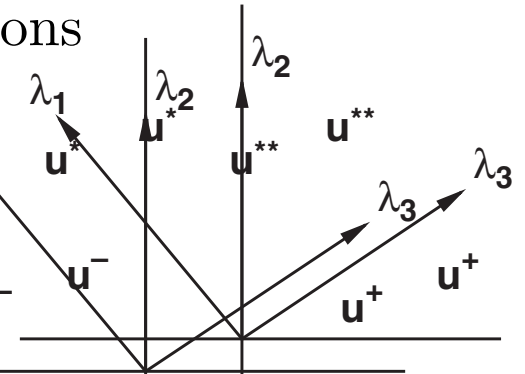
Linear systems and fluxes

So for the 3-wave problem we have

$$\lambda Q^-(\mathbf{u}^* - \mathbf{u}^-) + [(\Pi \mathbf{u})^* - (\Pi \mathbf{u})^-] = 0,$$

$$[(\Pi \mathbf{u})^* - (\Pi \mathbf{u})^{**}] = 0,$$

$$-\lambda Q^+(\mathbf{u}^{**} - \mathbf{u}^+) + [(\Pi \mathbf{u})^{**} - (\Pi \mathbf{u})^+] = 0,$$



and the numerical flux is given as

$$(\hat{\mathbf{n}} \cdot \mathcal{F})^* = (\Pi \mathbf{u})^* = (\Pi \mathbf{u})^{**},$$

This approach is general and yields the exact upwind fluxes -- but requires that the system can be solved !

Linear systems and fluxes -- an example

Consider

$$\frac{\partial \mathbf{q}}{\partial t} + \mathcal{A} \frac{\partial \mathbf{q}}{\partial x} = \frac{\partial}{\partial t} \begin{bmatrix} u \\ v \end{bmatrix} + \begin{bmatrix} a(x) & 0 \\ 0 & -a(x) \end{bmatrix} \frac{\partial}{\partial x} \begin{bmatrix} u \\ v \end{bmatrix} = 0,$$

Following the general approach, we have

$$\begin{aligned} a^- (\mathbf{q}^* - \mathbf{q}^-) + (\Pi \mathbf{q})^* - (\Pi \mathbf{q})^- &= 0, \\ -a^+ (\mathbf{q}^* - \mathbf{q}^+) + (\Pi \mathbf{q})^* - (\Pi \mathbf{q})^+ &= 0, \end{aligned}$$

with $(\Pi \mathbf{q})^\pm = \hat{\mathbf{n}} \cdot (\mathcal{A} \mathbf{q})^\pm = \hat{\mathbf{n}} \cdot \begin{bmatrix} a^\pm & 0 \\ 0 & -a^\pm \end{bmatrix} \begin{bmatrix} u^\pm \\ v^\pm \end{bmatrix} = \hat{\mathbf{n}} \cdot \begin{bmatrix} a^\pm u^\pm \\ -a^\pm v^\pm \end{bmatrix}.$

Solving this yields

$$(\Pi \mathbf{q})^* = \frac{2a^+ a^-}{a^+ + a^-} \hat{\mathbf{n}} \cdot \left(\begin{bmatrix} \{\{u\}\} \\ -\{\{v\}\} \end{bmatrix} + \frac{1}{2} \begin{bmatrix} \llbracket u \rrbracket \\ \llbracket v \rrbracket \end{bmatrix} \right),$$

Intermediate
velocity

$$a^* = \frac{2a^- a^+}{a^+ + a^-},$$

Linear systems and fluxes -- an example

Consider Maxwell's equations

$$\begin{bmatrix} \varepsilon(x) & 0 \\ 0 & \mu(x) \end{bmatrix} \frac{\partial}{\partial t} \begin{bmatrix} E \\ H \end{bmatrix} + \begin{bmatrix} 0 & 1 \\ 1 & 0 \end{bmatrix} \frac{\partial}{\partial x} \begin{bmatrix} E \\ H \end{bmatrix} = 0.$$

The exact same approach leads to

$$H^* = \frac{1}{\{\{Z\}\}} \left(\{\{ZH\}\} + \frac{1}{2} \llbracket E \rrbracket \right), \quad E^* = \frac{1}{\{\{Y\}\}} \left(\{\{YE\}\} + \frac{1}{2} \llbracket H \rrbracket \right),$$

Now assume smooth materials:

$$H^* = \{\{H\}\} + \frac{Y}{2} \llbracket E \rrbracket, \quad E^* = \{\{E\}\} + \frac{Z}{2} \llbracket H \rrbracket,$$

We have recovered the LF flux!

$$Z^\pm = \sqrt{\frac{\mu^\pm}{\varepsilon^\pm}} = (Y^\pm)^{-1},$$
$$\frac{Y}{\varepsilon} = \frac{Z}{\mu} = \frac{1}{\sqrt{\varepsilon\mu}} = c$$

An example

Consider Maxwell's equations

$$\varepsilon(x) \frac{\partial E}{\partial t} = -\frac{\partial H}{\partial x}, \quad \mu(x) \frac{\partial H}{\partial t} = -\frac{\partial E}{\partial x},$$

On the DG form

$$\begin{aligned} \frac{d\mathbf{E}_h^k}{dt} + \frac{1}{J^k \varepsilon^k} \mathcal{D}_r \mathbf{H}_h^k &= \frac{1}{J^k \varepsilon^k} \mathcal{M}^{-1} \left[\boldsymbol{\ell}^k(x) (H_h^k - H^*) \right]_{x_l^k}^{x_r^k} \\ &= \frac{1}{J^k \varepsilon^k} \mathcal{M}^{-1} \oint_{x_l^k}^{x_r^k} \hat{\mathbf{n}} \cdot (H_h^k - H^*) \boldsymbol{\ell}^k(x) dx, \end{aligned}$$

with the flux

$$H^- - H^* = \frac{1}{2\{\{Z\}\}} (Z^+ \llbracket H \rrbracket - \llbracket E \rrbracket),$$

$$E^- - E^* = \frac{1}{2\{\{Y\}\}} (Y^+ \llbracket E \rrbracket - \llbracket H \rrbracket),$$

An example

MaxwellRHS1D.m

```
function [rhsE, rhsH] = MaxwellRHS1D(E,H,eps,mu)
```

```
% function [rhsE, rhsH] = MaxwellRHS1D(E,H,eps,mu)  
% Purpose : Evaluate RHS flux in 1D Maxwell
```

```
Globals1D;
```

```
% Compute impedance  
Zimp = sqrt(mu./eps);
```

```
% Define field differences at faces
```

```
dE = zeros(Nfp*Nfaces,K); dE(:) = E(vmapM)-E(vmapP);
```

```
dH = zeros(Nfp*Nfaces,K); dH(:) = H(vmapM)-H(vmapP);
```

```
ZimpM = zeros(Nfp*Nfaces,K); ZimpM(:) = Zimp(vmapM);
```

```
ZimpP = zeros(Nfp*Nfaces,K); ZimpP(:) = Zimp(vmapP);
```

```
YimpM = zeros(Nfp*Nfaces,K); YimpM(:) = 1./ZimpM(:);
```

```
YimpP = zeros(Nfp*Nfaces,K); YimpP(:) = 1./ZimpP(:);
```

```
% Homogeneous boundary conditions, Ez=0
```

```
Ebc = -E(vmapB); dE (mapB) = E(vmapB) - Ebc;
```

```
Hbc = H(vmapB); dH (mapB) = H(vmapB) - Hbc;
```

```
% evaluate upwind fluxes
```

```
fluxE = 1./(ZimpM + ZimpP).*(nx.*ZimpP.*dH - dE);
```

```
fluxH = 1./(YimpM + YimpP).*(nx.*YimpP.*dE - dH);
```

```
% compute right hand sides of the PDE's
```

```
rhsE = (-rx.*(Dr*H) + LIFT*(Fscale.*fluxE))./eps;
```

```
rhsH = (-rx.*(Dr*E) + LIFT*(Fscale.*fluxH))./mu;
```

```
return
```

Impedance

Compute field jumps

Compute interface impedance

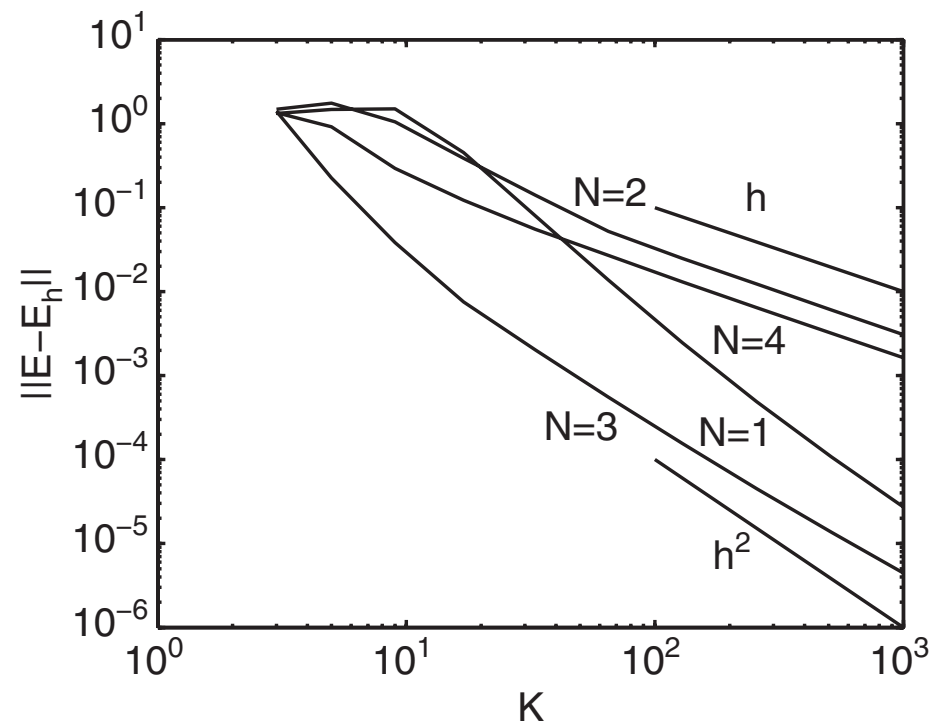
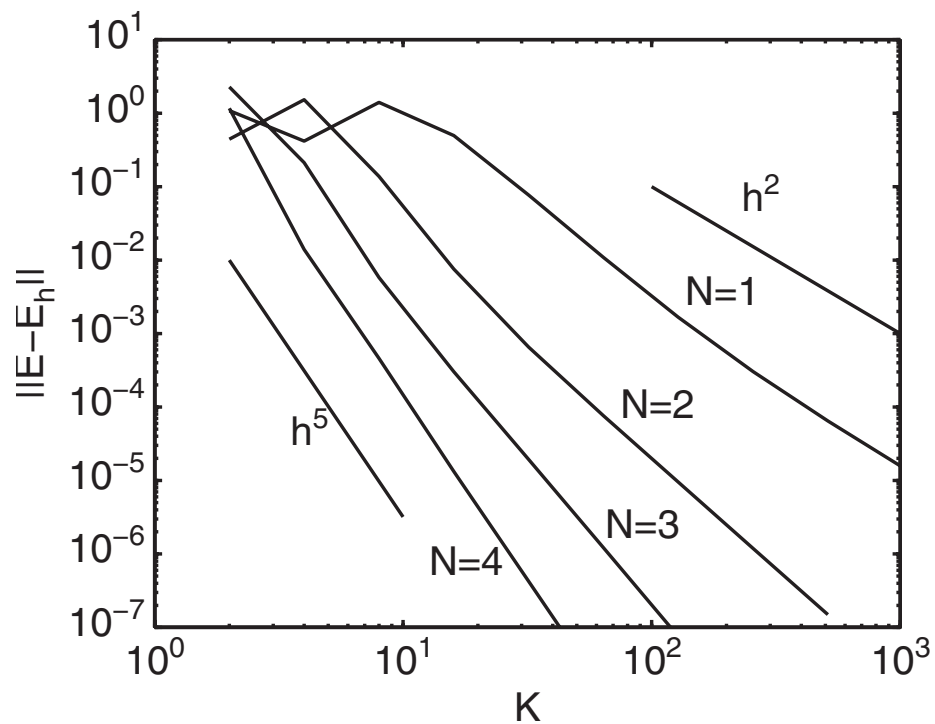
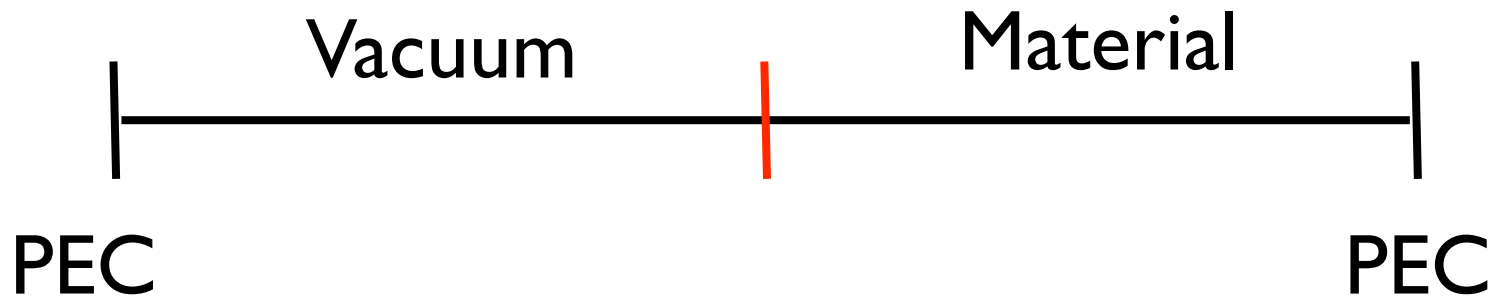
Boundary conditions

Complete fluxes

Complete computation

An example

Test example is cavity problem



Lets move on

At this point we have a good understanding of stability for linear problems -- through the flux.

Lets now look at accuracy in more detail.

Recall

$$\Omega \simeq \Omega_h = \bigcup_{k=1}^K D^k, \quad u(x, t) \simeq u_h(x, t) = \bigoplus_{k=1}^K u_h^k(x, t),$$

we assume the local solution to be

$$x \in D^k = [x_l^k, x_r^k] : u_h^k(x, t) = \sum_{n=1}^{N_p} \hat{u}_n^k(t) \psi_n(x) = \sum_{i=1}^{N_p} u_h^k(x_i^k, t) \ell_i^k(x).$$

modal basis

nodal basis

Local approximation

To simplify matters, introduce local affine mapping

$$x \in D^k : x(r) = x_l^k + \frac{1+r}{2} h^k, \quad h^k = x_r^k - x_l^k, \quad r \in [-1, 1]$$

We have already introduced the Legendre polynomials

$$u(r) \simeq u_h(r) = \sum_{n=1}^{N_p} \hat{u}_n \tilde{P}_{n-1}(r) = \sum_{i=1}^{N_p} u(r_i) \ell_i(r),$$

$$\mathbf{u} = \mathcal{V} \hat{\mathbf{u}}, \quad \mathcal{V}^T \ell(r) = \tilde{\mathbf{P}}(r), \quad \mathcal{V}_{ij} = \tilde{P}_j(r_i).$$

and r_i are the Legendre Gauss Lobatto points:

It is robust -- **but is it accurate ?**

A second look at approximation

We will need a little more notation

Regular energy norms

$$\|u\|_{\Omega}^2 = \int_{\Omega} u^2 d\mathbf{x} \quad \|u\|_{\Omega,h}^2 = \sum_{k=1}^K \|u\|_{\mathbf{D}^k}^2, \quad \|u\|_{\mathbf{D}^k}^2 = \int_{\mathbf{D}^k} u^2 d\mathbf{x}.$$

Sobolev norms

$$\|u\|_{\Omega,q}^2 = \sum_{|\alpha|=0}^q \|u^{(\alpha)}\|_{\Omega}^2, \quad \|u\|_{\Omega,q,h}^2 = \sum_{k=1}^K \|u\|_{\mathbf{D}^k,q}^2, \quad \|u\|_{\mathbf{D}^k,q}^2 = \sum_{|\alpha|=0}^q \|u^{(\alpha)}\|_{\mathbf{D}^k}^2,$$

Semi-norms

$$|u|_{\Omega,q,h}^2 = \sum_{k=1}^K |u|_{\mathbf{D}^k,q}^2, \quad |u|_{\mathbf{D}^k,q}^2 = \sum_{|\alpha|=q} \|u^{(\alpha)}\|_{\mathbf{D}^k}^2.$$

Approximation theory

Recall

$$\Omega \simeq \Omega_h = \bigcup_{k=1}^K D^k, \quad u(x, t) \simeq u_h(x, t) = \bigoplus_{k=1}^K u_h^k(x, t),$$

we assume the local solution to be

$$x \in D^k = [x_l^k, x_r^k] : u_h^k(x, t) = \sum_{n=1}^{N_p} \hat{u}_n^k(t) \psi_n(x) = \sum_{i=1}^{N_p} u_h^k(x_i^k, t) \ell_i^k(x).$$

The question is in what sense is $u(x, t) \simeq u_h(x, t)$

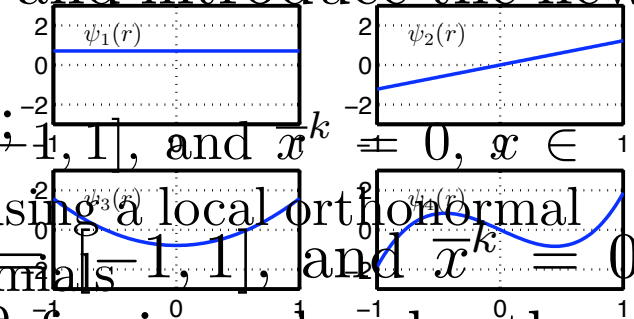
We have observed improved accuracy in two ways

- Increase K/decrease h
- Increase N

Approximation theory

Let us assume all elements have size h and consider

$$v(r) = u(hr) = u(x);$$



We consider expansions as

$$v_h(r) = \sum_{n=0}^N \hat{v}_n \tilde{P}_n(r), \quad \tilde{P}_n(r) = \frac{P_n(r)}{\sqrt{\gamma_n}}, \quad \gamma_n = \frac{2}{2n+1}. \quad \tilde{v}_n = \int_{-1}^1 v(r) \tilde{P}_n(r) dr.$$

Theorem 4.1. Assume that $v \in H^p(I)$ and that v_h represents a polynomial projection of order N . Then

$$\|v - v_h\|_{1,q} \leq N^{\rho-p} |v|_{1,p},$$

where

$$\rho = \begin{cases} \frac{3}{2}q, & 0 \leq q \leq 1 \\ 2q - \frac{1}{2}, & q \geq 1 \end{cases}$$

and $0 \leq q \leq p$.

Approximation theory

A sharper result can be obtained by using

Lemma 4.4. *If $v \in H^p(I)$, $p \geq 1$ then*

$$\|v^{(q)} - v_h^{(q)}\|_{1,0} \leq \left[\frac{(N+1-\sigma)!}{(N+1+\sigma-4q)!} \right]^{1/2} |v|_{1,\sigma},$$

where $\sigma = \min(N+1, p)$ and $q \leq p$.

Note that in the limit of $N \gg p$ we recover

$$\|v^{(q)} - v_h^{(q)}\|_{1,0} \leq N^{2q-p} |v|_{1,p},$$

A minor issues arises -- these results are based on projections and we are using interpolations ?

Approximation theory

We consider

$$v_h(r) = \sum_{n=0}^N \hat{v}_n \tilde{P}_n(r), \quad \tilde{v}_h(r) = \sum_{n=0}^N \tilde{v}_n \tilde{P}_n(r), \quad v = \mathcal{V}\hat{v},$$

interpolation projection

Compare the two

$$(\mathcal{V}\hat{v})_i = v_h(r_i) = \sum_{n=0}^{\infty} \tilde{v}_n \tilde{P}_n(r_i) = \sum_{n=0}^N \tilde{v}_n \tilde{P}_n(r_i) + \sum_{n=N+1}^{\infty} \tilde{v}_n \tilde{P}_n(r_i),$$

$$\mathcal{V}\hat{v} = \mathcal{V}\tilde{v} + \sum_{n=N+1}^{\infty} \tilde{v}_n \tilde{P}_n(\mathbf{r}),$$

$$v_h(r) = \tilde{v}_h(r) + \tilde{\mathbf{P}}^T(r) \mathcal{V}^{-1} \sum_{n=N+1}^{\infty} \tilde{v}_n \tilde{P}_n(\mathbf{r}).$$

Approximation theory

Consider this term

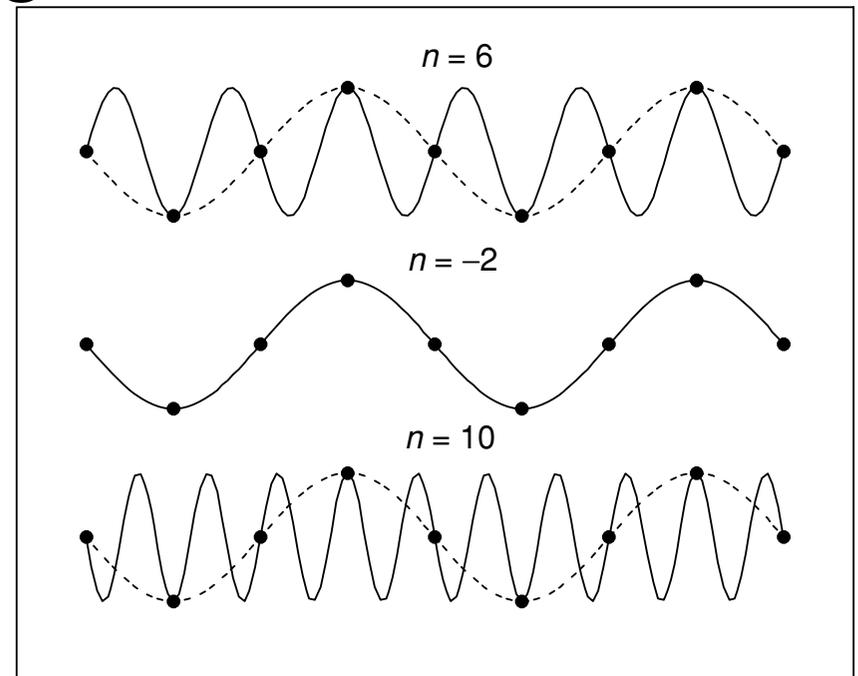
$$\tilde{\mathbf{P}}^T(\mathbf{r})\mathcal{V}^{-1} \sum_{n=N+1}^{\infty} \tilde{v}_n \tilde{P}_n(\mathbf{r}) = \sum_{n=N+1}^{\infty} \tilde{v}_n \left(\tilde{\mathbf{P}}^T(\mathbf{r})\mathcal{V}^{-1} \tilde{P}_n(\mathbf{r}) \right),$$

$$\tilde{\mathbf{P}}^T(\mathbf{r})\mathcal{V}^{-1} \tilde{P}_n(\mathbf{r}) = \sum_{l=0}^N \tilde{p}_l \tilde{P}_l(\mathbf{r}), \quad \mathcal{V}\tilde{\mathbf{p}} = \tilde{P}_n(\mathbf{r}),$$

Caused by interpolation of high-frequency unresolved modes

Aliasing

Caused by the grid



Approximation theory

This has a some impact on the accuracy

Theorem 4.5. *Assume that $v \in H^p(I)$, $p > \frac{1}{2}$, and that v_h represents a polynomial interpolation of order N . Then*

$$\|v - v_h\|_{I,q} \leq N^{2q-p+1/2} |v|_{I,p},$$

where $0 \leq q \leq p$.

To also account for the cell size we have

Theorem 4.7. *Assume that $u \in H^p(D^k)$ and that u_h represents a piecewise polynomial approximation of order N . Then*

$$\|u - u_h\|_{\Omega,q,h} \leq Ch^{\sigma-q} |u|_{\Omega,\sigma,h},$$

for $0 \leq q \leq \sigma$, and $\sigma = \min(N + 1, p)$.

Approximation theory

Combining everything, we have the general result

Theorem 4.8. *Assume that $u \in H^p(D^k)$, $p > 1/2$, and that u_h represents a piecewise polynomial interpolation of order N . Then*

$$\|u - u_h\|_{\Omega, q, h} \leq C \frac{h^{\sigma - q}}{N^{p - 2q - 1/2}} |u|_{\Omega, \sigma, h},$$

for $0 \leq q \leq \sigma$, and $\sigma = \min(N + 1, p)$.

with $h = \max_k h^k$

Lets summarize Part I

Fluxes:

✓ For linear systems, we can derive exact upwind fluxes using Rankine-Hugoniot conditions.

Accuracy:

- ✓ Legendre polynomials are the right basis
- ✓ Local accuracy depends on elementwise smoothness
- ✓ Aliasing appears due to the grid but is under control
- ✓ For smooth problems, we have a spectral method
- ✓ Convergence can be recovered in two ways
 - ✓ Increase N
 - ✓ Decrease h

Convergence of the solution at all times ?

Lecture 3

- ✓ Let's briefly recall what we know
- ✓ Why high-order methods ?
- ✓ Part I:
 - ✓ Constructing fluxes for linear systems
 - ✓ Approximation theory on the interval
- ✓ Part II:
 - ✓ Convergence and error estimates
 - ✓ Dispersive properties
 - ✓ Discrete stability and how to overcome

Lets recall convergence etc

We consider the system

$$\frac{\partial \mathbf{u}}{\partial t} + \mathcal{A} \frac{\partial \mathbf{u}}{\partial x} = 0,$$

which we assume is **wellposed** in the sense

$$\|\mathbf{u}(t)\|_{\Omega} \leq C \exp(\alpha t) \|\mathbf{u}(0)\|_{\Omega}.$$

The semi-discrete scheme is given as

$$\frac{d\mathbf{u}_h}{dt} + \mathcal{L}_h \mathbf{u}_h = 0.$$

Inserting the exact solution \mathbf{u} into the scheme yields

$$\frac{d\mathbf{u}}{dt} + \mathcal{L}_h \mathbf{u} = \mathcal{T}(\mathbf{u}(x, t)),$$

truncation error

Convergence and all that

Let us introduce the error

$$\varepsilon(\boldsymbol{x}, t) = \boldsymbol{u}(\boldsymbol{x}, t) - \boldsymbol{u}_h(\boldsymbol{x}, t),$$

What we really seek is convergence

$$\forall t \in [0, T] : \lim_{\text{dof} \rightarrow \infty} \|\varepsilon(t)\|_{\Omega, h} \rightarrow 0.$$

This is often a little complicated to get to due to the requirement for all t .

Let us get to it in a different way.

Convergence and all that

Let us consider the error equation

$$\frac{d}{dt}\boldsymbol{\varepsilon} + \mathcal{L}_h\boldsymbol{\varepsilon} = \mathcal{T}(\mathbf{u}(\mathbf{x}, t)),$$

The solution is given as

$$\boldsymbol{\varepsilon}(t) - \exp(-\mathcal{L}_h t)\boldsymbol{\varepsilon}(0) = \int_0^t \exp(\mathcal{L}_h(s-t))\mathcal{T}(\mathbf{u}(s))ds,$$

Now consider

$$\|\boldsymbol{\varepsilon}(t)\|_{\Omega,h} \leq \|\exp(-\mathcal{L}_h t)\boldsymbol{\varepsilon}(0)\|_{\Omega,h} + \left\| \int_0^t \exp(\mathcal{L}_h(s-t))\mathcal{T}(\mathbf{u}(s))ds \right\|_{\Omega,h}$$

$$\left\| \int_0^t \exp(\mathcal{L}_h(s-t))\mathcal{T}(\mathbf{u}(s))ds \right\|_{\Omega,h} \leq \int_0^t \|\exp(\mathcal{L}_h(s-t))\|_{\Omega,h} \|\mathcal{T}(\mathbf{u}(s))\|_{\Omega,h} ds,$$

Convergence and all that

So if we require **consistency**

$$\begin{cases} \lim_{\text{dof} \rightarrow \infty} \|\boldsymbol{\varepsilon}(0)\|_{\Omega, h} = 0, \\ \lim_{\text{dof} \rightarrow \infty} \|\mathcal{T}(\mathbf{u}(t))\|_{\Omega, h} = 0 \end{cases}$$

and **stability**

$$\lim_{\text{dof} \rightarrow \infty} \|\exp(-\mathcal{L}_h t)\|_{\Omega, h} \leq C_h \exp(\alpha_h t), \quad t \geq 0,$$

we obtain **convergence**

$$\forall t \in [0, T] : \lim_{\text{dof} \rightarrow \infty} \|\boldsymbol{\varepsilon}(t)\|_{\Omega, h} \rightarrow 0.$$

This is of course part of the celebrated Lax-Richtmyer equivalence theorem

Convergence and all that

Recall

$$\frac{\partial u}{\partial t} + a \frac{\partial u}{\partial x} = 0,$$

for which we proved stability as

$$\frac{1}{2} \frac{d}{dt} \|u_h\|_{\Omega, h}^2 \leq c \|u_h\|_{\Omega, h}^2,$$

This generalizes easily to systems when upwinding is used on the characteristic variables.

Combining this with the accuracy analysis yields

$$\|u - u_h\|_{\Omega, h} \leq \frac{h^N}{N^{p-5/2}} |u|_{\Omega, p, h},$$

but we observed

$$\|u(T) - u_h(T)\|_{\Omega, h} \leq h^{N+1} (C_1 + TC_2).$$

Error estimates

To get closer to the observed behavior, we need to be a little more careful.

Define $\mathcal{B}(u, \phi) = (u_t, \phi)_{\Omega} + a(u_x, v)_{\Omega} = 0$

we have $\mathcal{B}(u, u) = 0 = \frac{1}{2} \frac{d}{dt} \|u\|_{\Omega}^2;$

For two different solutions we have

$$\varepsilon(t) = u_1(t) - u_2(t)$$

$$\frac{1}{2} \frac{d}{dt} \|\varepsilon\|_{\Omega}^2 = 0, \quad \longrightarrow \quad \|\varepsilon(T)\|_{\Omega} = \|u_1(0) - u_2(0)\|_{\Omega},$$

Error estimates

We will now mimic this for the semi-discrete problem

$$\mathcal{B}_h(u_h, \phi_h) = ((u_h)_t, \phi_h)_{\Omega, h} + a((u_h)_x, \phi_h)_{\Omega, h} - (\hat{\mathbf{n}} \cdot (au_h - (au)^*), \phi_h)_{\partial\Omega, h} = 0,$$

Let us use a central flux

$$(au)^* = \{\{au\}\},$$

to obtain

$$\mathcal{B}_h(u_h, \phi_h) = ((u_h)_t, \phi_h)_{\Omega, h} + a((u_h)_x, \phi_h)_{\Omega, h} - \frac{1}{2}(\llbracket au_h \rrbracket, \phi_h)_{\partial\Omega, h} = 0.$$

Observe

$$\mathcal{B}_h(u, \phi_h) = 0, \quad \longrightarrow \quad \mathcal{B}_h(\varepsilon, \phi_h) = 0, \quad \varepsilon = u - u_h.$$

Using

$$\mathcal{B}_h(\varepsilon_h, \varepsilon_h) = \frac{1}{2} \frac{d}{dt} \|\varepsilon_h\|_{\Omega, h}^2.$$

Error estimates

Now consider

$$\frac{1}{2} \frac{d}{dt} \|\varepsilon_N\|_{\Omega, h}^2 = \mathcal{B}_h(\mathcal{P}_N u - u, \varepsilon_h),$$

one proves (with some work)

$$\begin{aligned} |\mathcal{B}_h(u - \mathcal{P}_N u, \varepsilon_h)| &\leq \frac{1}{2} ((\{\{a q\}\}, \{\{a q\}\})_{\partial\Omega, h} + (\varepsilon_h, \varepsilon_h)_{\partial\Omega, h}) \\ &\leq C|a|h^{2\sigma-1} \|u\|_{\Omega, h, \sigma+1}^2, \end{aligned}$$

 $\frac{d}{dt} \|\varepsilon_h\|_{\Omega, h}^2 \leq C|a|h^{2\sigma-1} \|u\|_{\Omega, h, \sigma+1}^2,$

 $\|\varepsilon_h(T)\| \leq (C_1 + C_2 T) h^{N+1/2},$

Better -- but not quite there

Error estimates

The observe full order

$$\|u(T) - u_h(T)\|_{\Omega, h} \leq h^{N+1} (C_1 + TC_2).$$

is in fact a special case !

It only works when

- ✓ When full upwinding on all characteristic variables are used
- ✓ Proof is only valid for the linear case
- ✓ Proof relies on 1D superconvergence results

In spite of this, optimal convergence is observed in many problems - why ?

Why often optimal anyway ?

Assume stability

$$\lim_{\text{dof} \rightarrow \infty} \|\exp(-\mathcal{L}_h t)\|_{\Omega, h} \leq C_h \exp(\alpha_h t), \quad t \geq 0,$$

Recall

$$\|\boldsymbol{\varepsilon}(t)\|_{\Omega, h} \leq \|\exp(-\mathcal{L}_h t) \boldsymbol{\varepsilon}(0)\|_{\Omega, h} + \left\| \int_0^t \exp(\mathcal{L}_h(s-t)) \mathcal{T}(\mathbf{u}(s)) ds \right\|_{\Omega, t}$$

Error in I.C.

Error
accumulation

$$\|u - u_h\|_{\Omega, q, h} \leq C \frac{h^{\sigma-q}}{N^{p-2q-1/2}} |u|_{\Omega, \sigma, h},$$

$$\sigma = \min(N + 1, p).$$

Dispersive properties

Consider again

$$\begin{aligned} \frac{\partial u}{\partial t} + a \frac{\partial u}{\partial x} &= 0, \\ u(x, 0) &= \exp(ilx), \end{aligned} \quad \Rightarrow \quad u(x, t) = \exp(i(lx - \omega t)),$$

The scheme is given as

$$\begin{aligned} \frac{h}{2} \mathcal{M} \frac{d\mathbf{u}_h^k}{dt} + a \mathcal{S} \mathbf{u}^k &= \mathbf{e}_N [(au_h^k) - (au_h^k)^*]_{x_r^k} - \mathbf{e}_0 [(au_h^k) - (au_h^k)^*]_{x_l^k}, \\ (au)^* &= \{\{au\}\} + |a| \frac{1 - \alpha}{2} \llbracket u \rrbracket. \end{aligned}$$

Look for solutions of the form

$$\mathbf{u}_h^k(x^k, t) = \mathbf{U}_h^k \exp[i(lx^k - \omega t)],$$

Dispersive properties

We recover

$$\begin{aligned} & [2\mathcal{S} - \alpha \mathbf{e}_N (\mathbf{e}_N^T - \exp(iL(N+1))\mathbf{e}_0^T) \\ & + (2 - \alpha)\mathbf{e}_0 (\mathbf{e}_0^T - \exp(-iL(N+1))\mathbf{e}_N^T)] \mathbf{U}_h^k = i\Omega \mathcal{M} \mathbf{U}_h^k. \end{aligned}$$

Where

$$L = \frac{lh}{N+1} = \frac{2\pi}{\lambda} \frac{h}{N+1} = 2\pi p^{-1}, \quad \Omega = \frac{\omega h}{a},$$

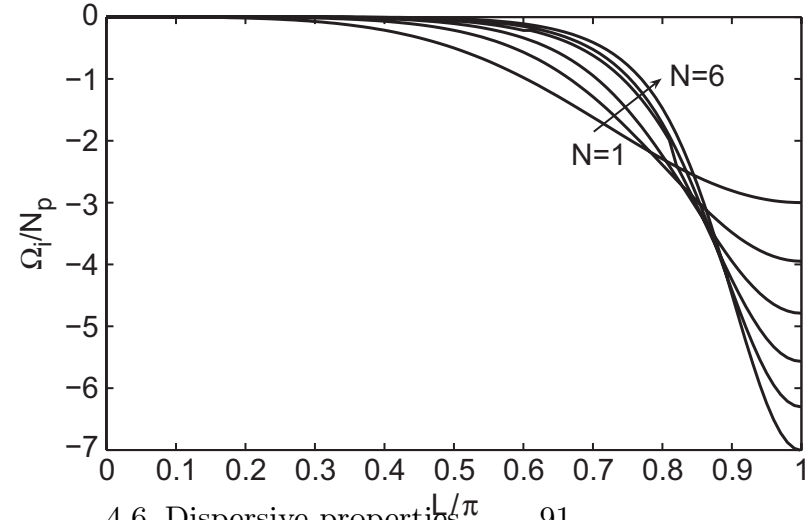
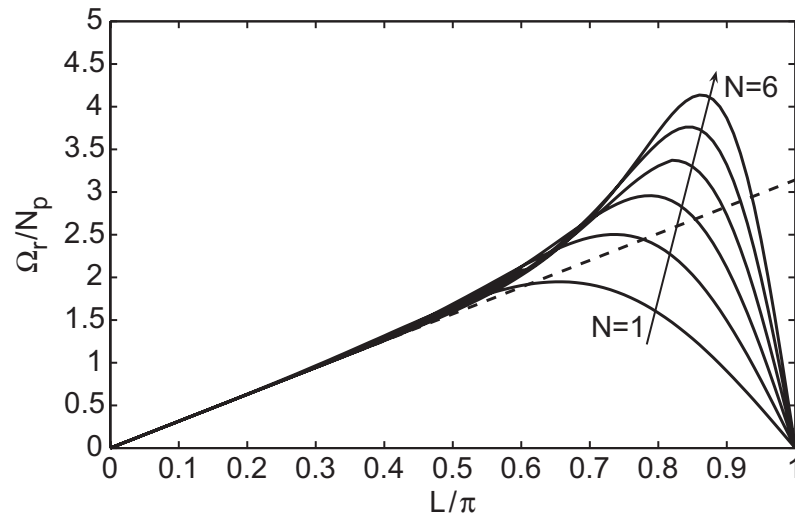
$$p = \frac{\lambda}{h/(N+1)} = \text{DoF per wavelength}$$

So for a fixed L we solve the eigenvalue problem

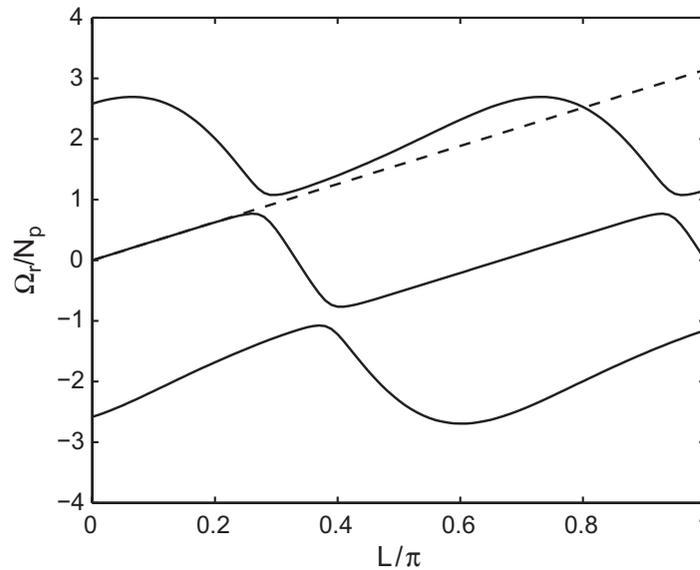
.. and the eigenvalue will tell us how the wave propagates

Dispersive properties

Upwind fluxes



Central fluxes



N=2

Dispersive properties

There are some analytic results available (upwind)

$$\left| \mathcal{R}(\tilde{lh}) - \mathcal{R}(lh) \right| \simeq \frac{1}{2} \left[\frac{N!}{(2N+1)!} \right]^2 (lh)^{2N+3},$$

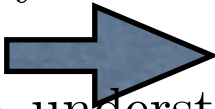
$$\left| \mathcal{I}(\tilde{lh}) \right| \simeq \frac{1}{2} \left[\frac{N!}{(2N+1)!} \right]^2 (1-\alpha)^{(-1)^N} (lh)^{2N+2},$$

The dispersive accuracy is excellent!

Define the relative phase error

$$\rho_N = \left| \frac{\exp(ilh) - \exp(i\tilde{lh})}{\exp(ilh)} \right|,$$

$$\rho_N \simeq \begin{cases} 2N+1 < lh - C(lh)^{1/3}, & \text{no convergence} \\ lh - o(lh)^{1/3} < 2N+1 < lh + o(lh)^{1/3}, & \mathcal{O}(N^{-1/3}) \text{ convergence} \\ 2N+1 \gg lh, & \mathcal{O}(hl/(2N+1))^{2N+2} \text{ convergence} \end{cases}$$

Convergence for $2 \simeq \frac{lh}{N+1} = 2\pi p^{-1};$  $p \geq \pi$,

Discrete stability

So far we have not done anything to discretize time.

$$\frac{\partial u}{\partial t} + a \frac{\partial u}{\partial x} = 0 \quad \Rightarrow \quad \frac{d\mathbf{u}_h}{dt} + \mathcal{L}_h \mathbf{u}_h = 0.$$

We shall consider the use of ERK methods

$$\mathbf{k}^{(1)} = \mathcal{L}_h (\mathbf{u}_h^n, t^n),$$

$$\mathbf{k}^{(2)} = \mathcal{L}_h \left(\mathbf{u}_h^n + \frac{1}{2} \Delta t \mathbf{k}^{(1)}, t^n + \frac{1}{2} \Delta t \right),$$

$$\mathbf{k}^{(3)} = \mathcal{L}_h \left(\mathbf{u}_h^n + \frac{1}{2} \Delta t \mathbf{k}^{(2)}, t^n + \frac{1}{2} \Delta t \right),$$

$$\mathbf{k}^{(4)} = \mathcal{L}_h \left(\mathbf{u}_h^n + \Delta t \mathbf{k}^{(3)}, t^n + \Delta t \right),$$

$$\mathbf{u}_h^{n+1} = \mathbf{u}_h^n + \frac{1}{6} \Delta t \left(\mathbf{k}^{(1)} + 2\mathbf{k}^{(2)} + 2\mathbf{k}^{(3)} + \mathbf{k}^{(4)} \right),$$

Discrete stability

and also a Low Storage form

$$\mathbf{p}^{(0)} = \mathbf{u}^n,$$

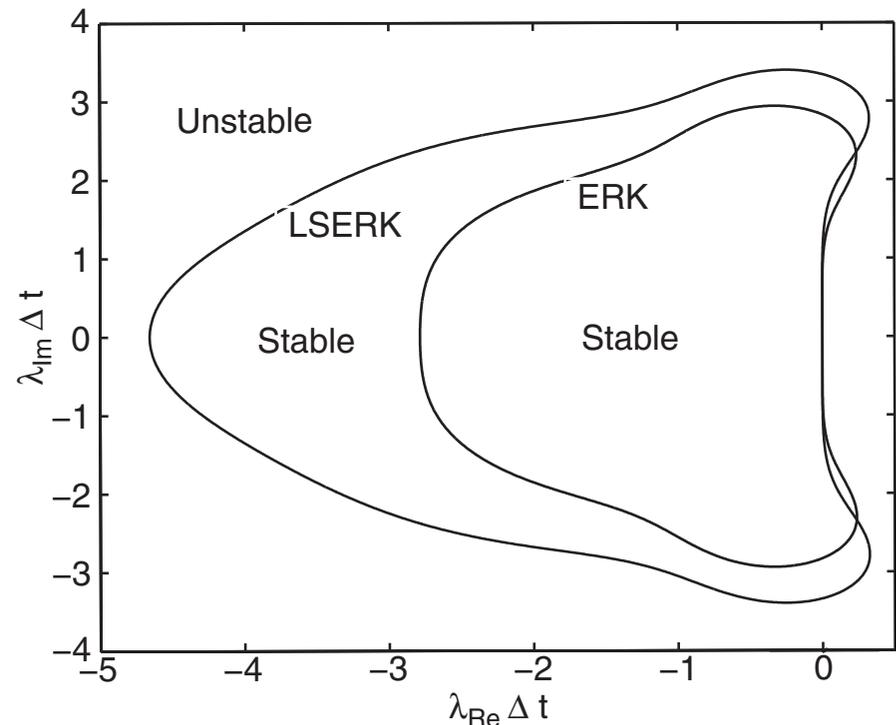
$$i \in [1, \dots, 5] : \begin{cases} \mathbf{k}^{(i)} = a_i \mathbf{k}^{(i-1)} + \Delta t \mathcal{L}_h (\mathbf{p}^{(i-1)}, t^n + c_i \Delta t), \\ \mathbf{p}^{(i)} = \mathbf{p}^{(i-1)} + b_i \mathbf{k}^{(i)}, \end{cases}$$

$$\mathbf{u}_h^{n+1} = \mathbf{p}^{(5)}.$$

Consider

$$u_t = \lambda u, \quad \text{Real}(\lambda) \leq 0,$$

The *stability region* defines the timestep that gives stability.



Discrete stability

Consider

$$\mathcal{L}_h = \frac{2a}{h} \mathcal{M}^{-1} [\mathcal{S} - \mathcal{E}],$$

We have

$$\begin{aligned} \frac{h^2}{4a^2} \|\mathcal{L}_h\|_1^2 &= \frac{h^2}{4a^2} \sup_{\|u_h\|=1} \|\mathcal{L}_h u_h\|_1^2 \\ &\leq \|\mathcal{D}_r\|_1^2 + \|\mathcal{M}^{-1} \mathcal{E}\|_1^2 + 2 \sup_{\|u_h\|=1} (\mathcal{D}_r u_h, \mathcal{M}^{-1} \mathcal{E} u_h)_1 \\ &\leq C_1 N^4 + C_2 N^2 + C_3 N^3 \leq C N^4, \end{aligned}$$

So we should expect

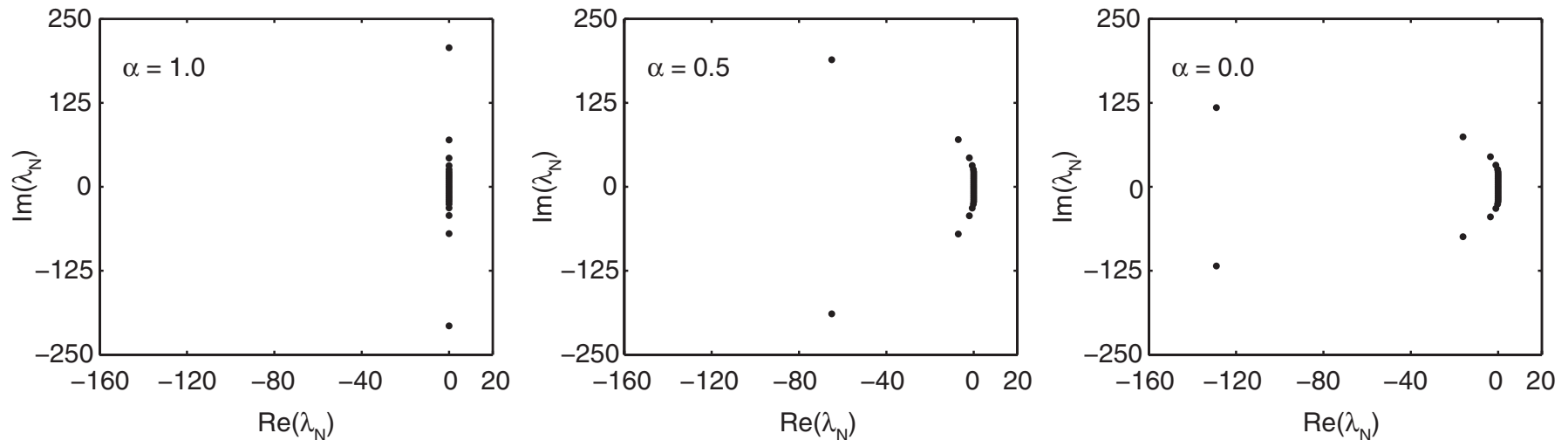
$$\|\mathcal{L}_h\|_{D^k} \leq C \frac{a}{h^k} N^2$$

Which would indicate

$$\Delta t \leq C \frac{h}{aN^2}$$

Discrete stability

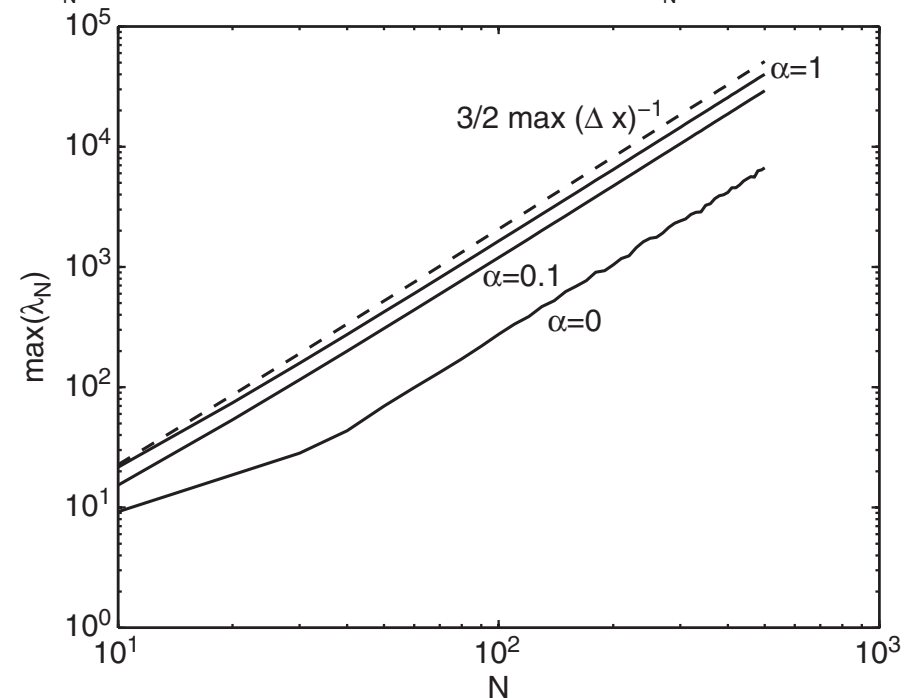
The structure also matters



The estimate

$$\Delta t \leq C \frac{h}{aN^2}$$

is sharp !



Discrete stability

General guidelines

$$\frac{\partial u}{\partial t} + a \frac{\partial u}{\partial x} = 0, \quad \Rightarrow \quad \Delta t \leq C \frac{1}{|a|} \min_{k,i} \frac{h^k}{2} (\Delta_i r),$$

$$\frac{\partial u}{\partial t} + \mathcal{A} \frac{\partial u}{\partial x} = 0, \quad \Rightarrow \quad \Delta t \leq C \frac{1}{\max(|\lambda(\mathcal{A})|)} \min_{k,i} \frac{h^k}{2} (\Delta_i r),$$

There are tricks to play to improve on this

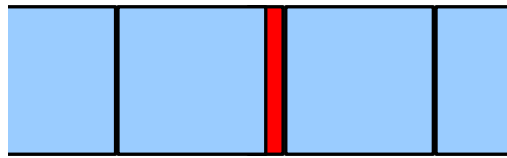
- ✓ Mappings to improve the scaling
- ✓ Covolume filtering techniques
- ✓ **Local time-stepping**

See text for a discussion of other methods

Local time-stepping

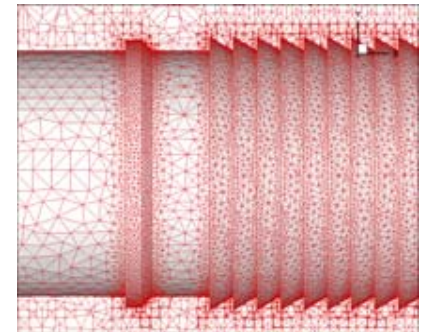
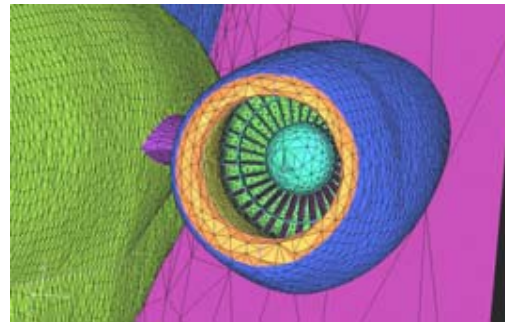
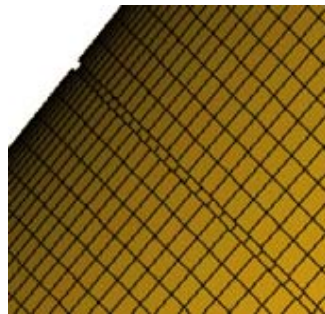


Problem: Small cells, even just one, cause a very small global time-step in an explicit scheme.



$$\Delta t \leq C \sqrt{\varepsilon \mu} \Delta x \simeq C_1 \sqrt{\varepsilon \mu} \frac{N^2}{h}$$

A significant problem for large scale complex applications



Old idea: take only time-steps required by local restrictions.

Old problems: accuracy and stability

Local time-stepping

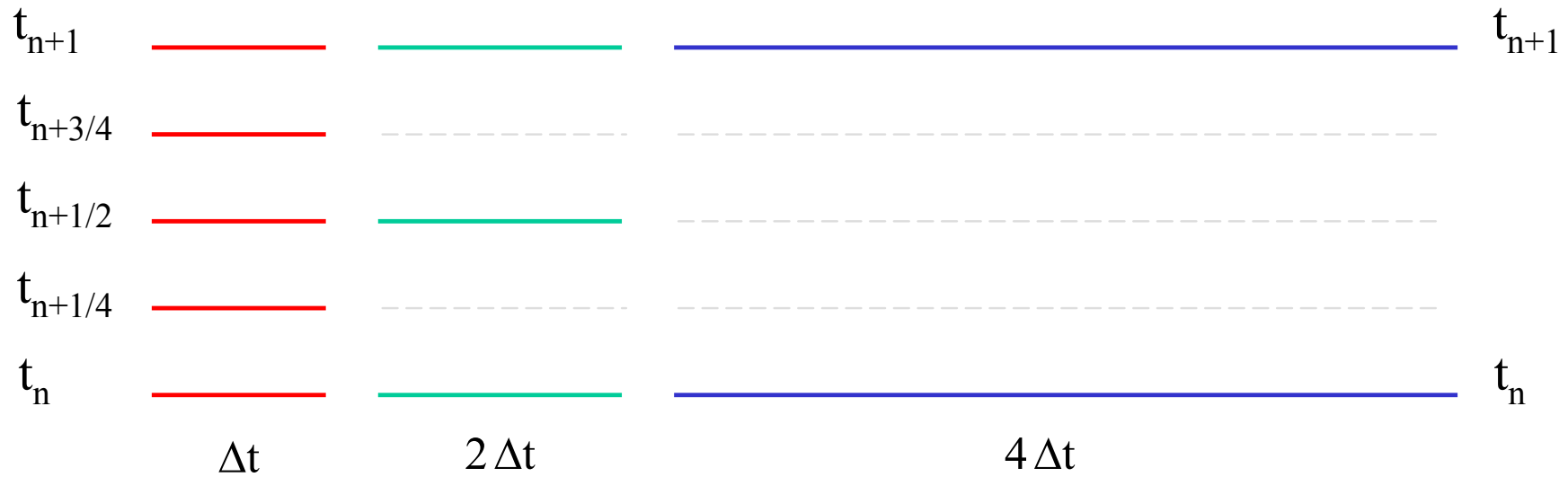


Substantial recent work by

Cohen, Grote, Lanteri, Piperno, Gassner, Munz etc

Most of the recent work is based on LF-like schemes,
restricted to 2nd order in time.

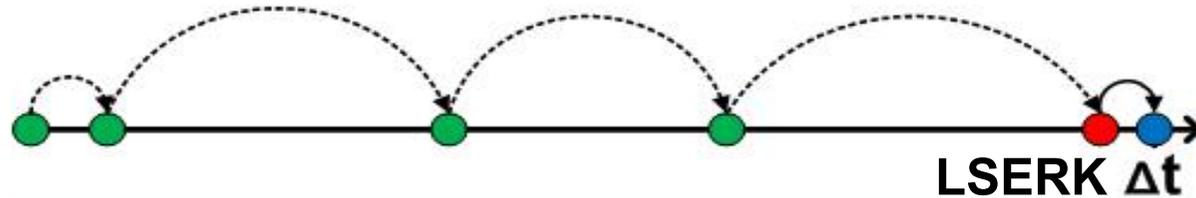
Layout for **multi-rate** local time-stepping



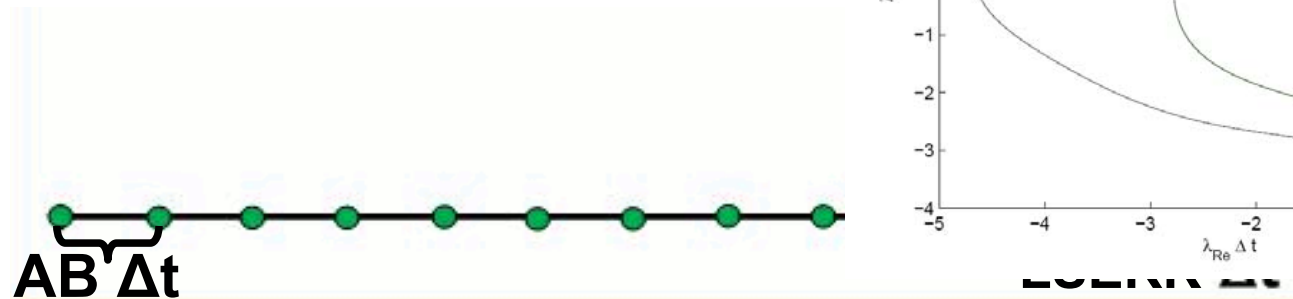
Local time-stepping



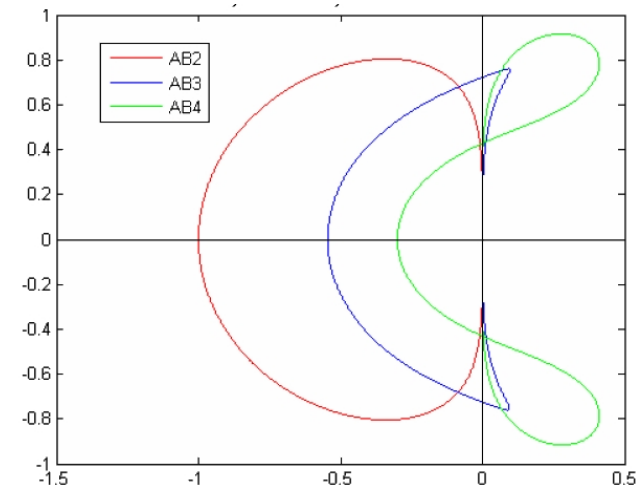
Recall the ERK scheme



We consider a multi-step scheme



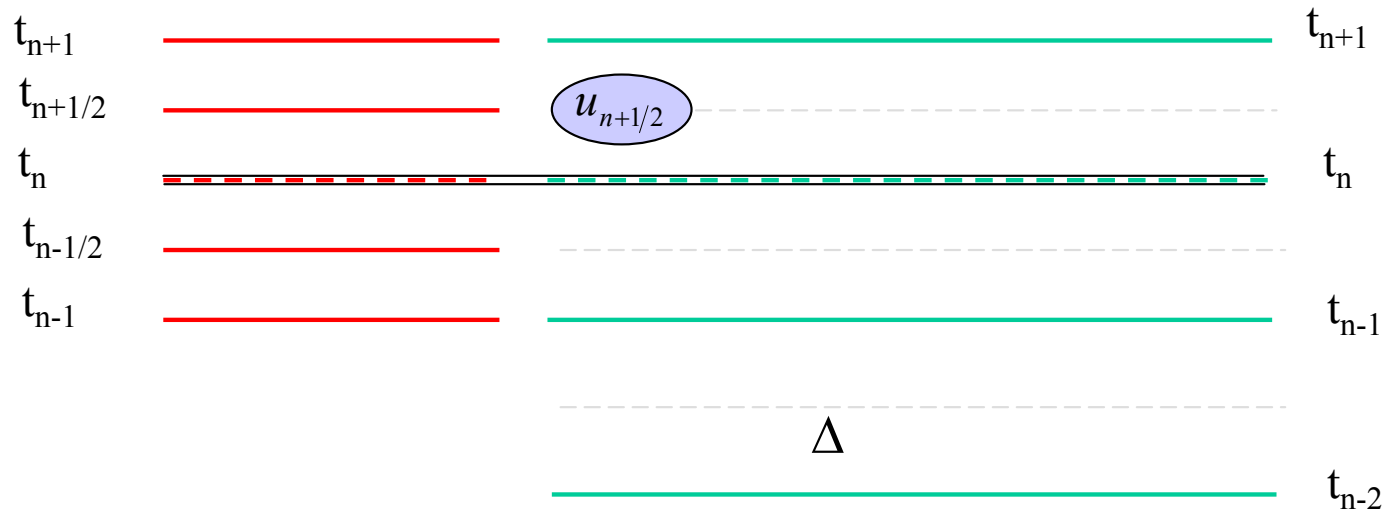
$$u_{n+1} = u_n + \frac{\Delta t}{12} [23F(u_n) - 16F(u_{n-1}) + 5F(u_{n-2})]$$



Local time-stepping



Challenge: Achieving this at high-order accuracy

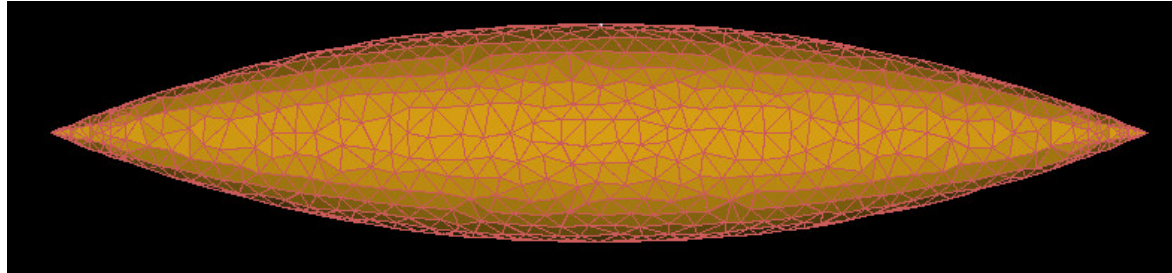


For all interior cells $u_{n+1} = u_n + \frac{\Delta t}{12} [23F(u_n) - 16F(u_{n-1}) + 5F(u_{n-2})]$

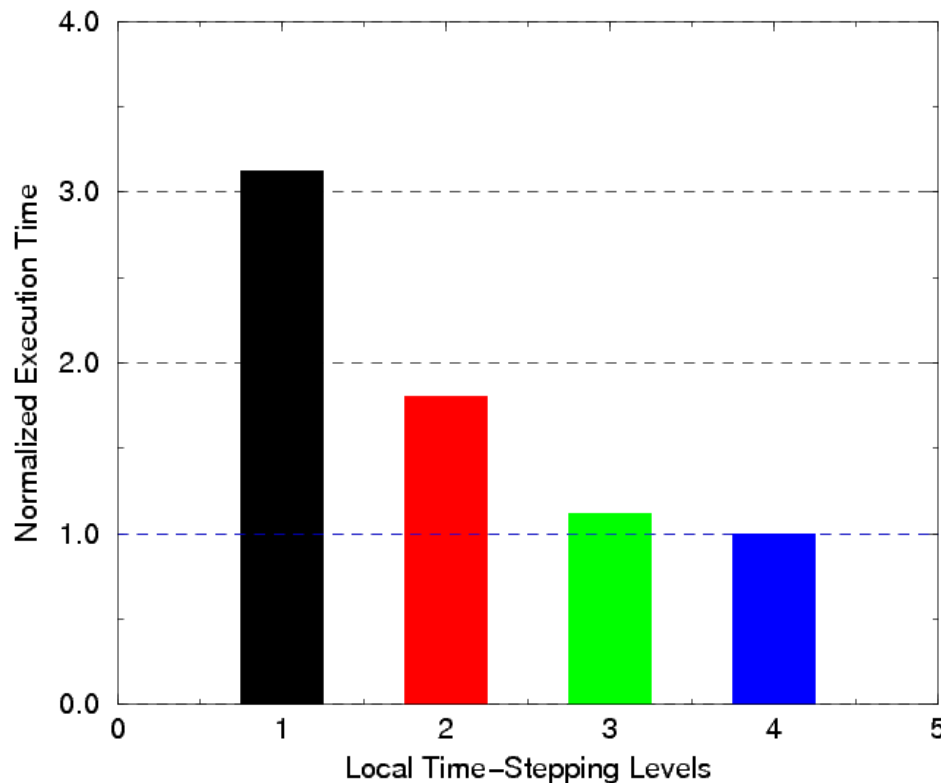
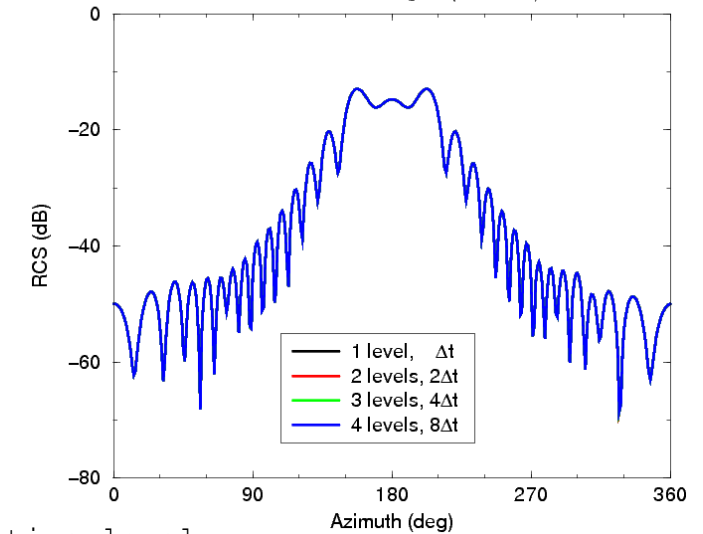
At interface cells $u_{n+1/2} = u_n + \frac{\Delta t}{12} [17F(u_n) - 7F(u_{n-1}) + 2F(u_{n-2})]$

This generalizes to many levels and arbitrary time-step fractions

Local time-stepping



Four Time-Level Local Time-Stepping
Bistatic RCS for Ogive (nose-on)



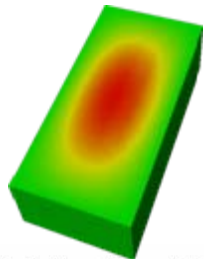
- One time level:
 - $N_o = 23742$
- Two time levels:
 - $N_o = 151$ (<1%)
 - $N_1 = 23591$ (99%)
- Three time levels:
 - $N_o = 151$ (<1%)
 - $N_1 = 1959$ (8%)
 - $N_2 = 21632$ (91%)
- Four time levels:
 - $N_o = 151$ (<1%)
 - $N_1 = 1959$ (8%)
 - $N_2 = 12622$ (53%)
 - $N_3 = 9010$ (38%)

Computations by
HyperComp Inc

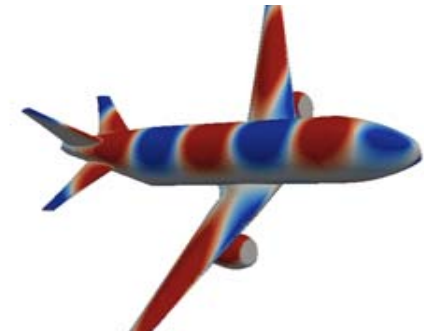
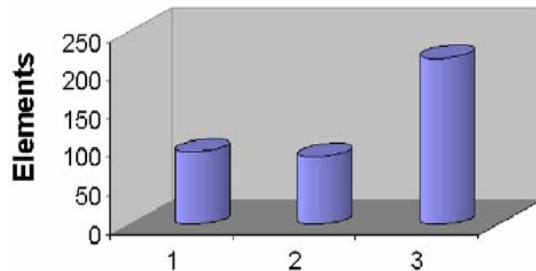
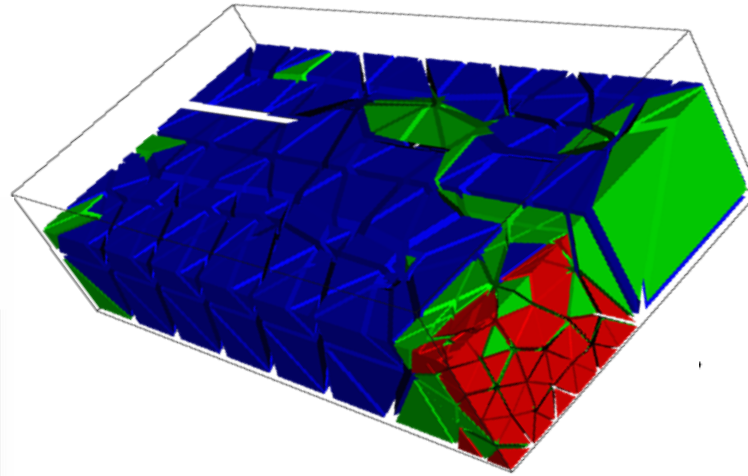
Local time-stepping



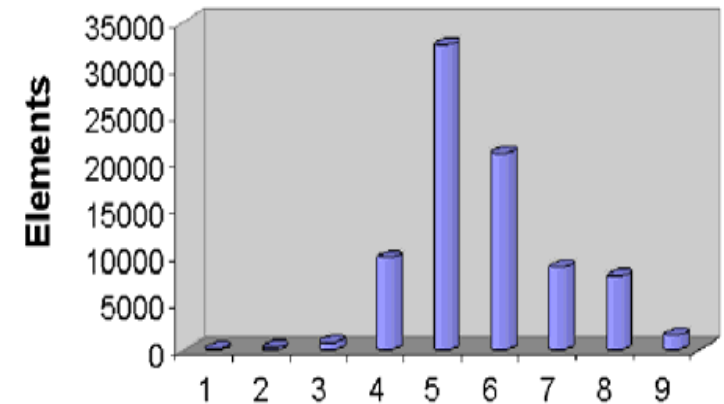
Segmentation is done in preprocessing



Level distribution 3D cavity



Level distribution airplane



Ideally suited for local DG scheme

Known problems:

No known stability proof

Time-step is not optimal (about 80%)

Local time-stepping



The potential speed up is considerable -- and the more complex the better !

Example	Simulation time with		
	Adams-Bashford (global time step)	Adams-Bashford (local time step)	LSERK (global time step)
Resonator	100%	59%	45%
3dB-Coupler	100%	29%	45%
Airplane	100%	15%	45%

Computations by Nico Godel, Hamburg

A brief summary

We now have a good understanding all key aspects of the DG-FEM scheme for linear first order problems

- We understand both **accuracy and stability** and what we can expect.
- The **dispersive properties** are excellent.
- The **discrete stability** is a little less encouraging.

A scaling like

$$\Delta t \leq C \frac{h}{aN^2}$$

is the Achilles Heel -- but there are ways!

... but what about nonlinear problems ?